

RSC Advances



This is an *Accepted Manuscript*, which has been through the Royal Society of Chemistry peer review process and has been accepted for publication.

Accepted Manuscripts are published online shortly after acceptance, before technical editing, formatting and proof reading. Using this free service, authors can make their results available to the community, in citable form, before we publish the edited article. This *Accepted Manuscript* will be replaced by the edited, formatted and paginated article as soon as this is available.

You can find more information about *Accepted Manuscripts* in the [Information for Authors](#).

Please note that technical editing may introduce minor changes to the text and/or graphics, which may alter content. The journal's standard [Terms & Conditions](#) and the [Ethical guidelines](#) still apply. In no event shall the Royal Society of Chemistry be held responsible for any errors or omissions in this *Accepted Manuscript* or any consequences arising from the use of any information it contains.

1 **Sampling of Dissolved Inorganic Sb^{III} by**
2 **Mercapto-Functionalized Silica-based Diffusive Gradients**
3 **in Thin-Films Technique**

4 Hong-Tao Fan^{1,*}, Ai-Juan Liu¹, Bing Jiang¹, Qing-Jie Wang¹, Tong Li¹, Cong-Cong Huang^{2,*}

5 ¹ Liaoning Provincial Key Laboratory of Chemical Separation Technology, Shenyang
6 University of Chemical Technology, Shenyang, 100142, Liaoning, China

7 ² Food Engineering, Shandong Business Institute, Yantai 264670, China

8 * Corresponding author

9 E-mail: 1183852624@qq.com (Hong-Tao Fan) and meiyueqinghe@163.com (Cong-Cong
10 Huang)

11 Tel.: +86-24-89383297

12 Fax: +86-24-83676698

13 **Abstract**

14 The mercapto-functionalized silica (MPS) diffusive gradients in thin-films (DGT) device, for
15 the first time, was characterized by the determination of dissolved inorganic Sb^{III}. The
16 performance of MPS–DGT was assessed by (1) determining the diffusion coefficient of Sb^{III}
17 in polyethersulfone membrane, (2) assessing an uptake efficiency and digestion efficiency of
18 MPS for Sb^{III}, (3) investigating the effect of pH, ionic strength (as NaNO₃) and foreign ions
19 on performance of MPS–DGT for Sb^{III} species, and (4) assessing the validation of MPS–DGT
20 for the measurement of dissolved inorganic Sb^{III} in spiked waters. The diffusion coefficient of
21 Sb^{III} measured in PES membrane by a diffusion cell was $(3.05 \pm 0.09) \times 10^{-6} \text{ cm}^2 \text{ s}^{-1}$. There was
22 a tendency toward higher adsorption affinity for Sb^{III} compared with the Sb^V. Mass vs. time
23 deployments of MPS–DGT at pH 6 (0.01 mol L⁻¹ NaNO₃) demonstrated linear uptake of Sb^{III}
24 ($R^2=0.9973$). The MPS–DGT was independent of ionic strength (0.001–0.7 mol L⁻¹ NaNO₃ at
25 pH 5) and pH (3–8, 0.01 mol L⁻¹ NaNO₃) for the measurement of Sb^{III}. The presence of
26 foreign ions (such as Ca^{II}, Mg^{II}, Cd^{II}, Zn^{II}, Cu^{II}, As^{III} and Sb^V) has no significant influence on
27 the uptake of Sb^{III} by MPS–DGT. MPS–DGT can quantitatively measure the concentration of
28 dissolved inorganic Sb^{III} in spiked etching wastewater. In spiked natural freshwater, the
29 concentration of dissolved inorganic Sb^{III} obtained by MPS–DGT is significant lower than the
30 concentration of added Sb^{III} due to the presence of natural organic matter (8.7 mg C L⁻¹)
31 which would have complexed a fraction of the added Sb^{III} and have changed the speciation of
32 added Sb^{III}. The MPS–DGT device can potentially be used as a tool of speciation
33 measurement for Sb^{III} in aqueous environments.

34 **Keywords:** Diffusive Gradients in Thin-Films, Speciation; Antimony

35 1. Introduction

36 Antimony (Sb) is listed as a priority pollutant by the U.S. Environmental Protection Agency
37 due to its toxicity.¹ Different species of Sb in environment may show great differences in
38 chemical behavior and is a critical factor influencing their toxicity.² Sb^{III} species are usually
39 more toxic than Sb^V.³ Determination of the chemical speciation of Sb in environment is
40 important to get additional information about its chemical forms, mobility, availability,
41 geochemical behavior and toxicity.⁴ It is essential to develop the reliable methods for
42 monitoring and sampling the different species of Sb in environmental samples.

43 The diffusive gradients in thin-films (DGT) technique has been developed by Davison and
44 Zhang⁵ and become one of the most promising in situ sampling and measurement techniques
45 for trace metals in natural waters, soils and sediments.⁶ The DGT device contains a diffusion
46 layer (e.g. polyacrylamide hydrogel,⁷ dialysis membrane,⁸ nylon membrane⁹ or
47 chromatography paper¹⁰) which allows solute species below a size threshold to pass and a
48 binding layer which is behind the diffusive layer.⁵ The binding layer usually comprises a
49 binding agent which can bind the metal species across a diffusion layer.⁵ Garmo and
50 co-workers investigate DGT device with a gel-layer incorporating chelex-100 resin as the
51 binding agent and a hydrated polyacrylamide gel as the diffusion gel (Chelex–DGT) for the
52 measurement of 55 elements, and find that Chelex-DGT is capable of measuring 24 elements
53 accurately, whereas, for the element of Sb^{III}, linear uptake with time is not observed by
54 Chelex–DGT indicating that this metal is not quantitatively collected by Chelex–100 resin
55 and can not be measured by Chelex–DGT.¹¹ Recently, precipitated ferrihydrite has been used
56 as a DGT binding agent for the measurement of Sb^V, As^V, V^V and Se^{VI}.¹² Panther and
57 co-workers reported a new DGT device using a titanium dioxide-based adsorbent as the
58 binding agent for the measurement of a variety of anionic species such as Sb^V, As^V, V^V, Mo^{VI}
59 and W^{VI}.¹³ However, the studies on the sampling and measuring of Sb^{III} by DGT technique in

60 water are still insufficient. Such constraint should be rectified by the incorporation of Sb
61 alternative binding agents. Previous researches have reported that the compounds containing
62 thiol groups have strong affinity for Sb^{III} ¹⁴ and can be used for the separation of Sb^{III} from the
63 mixed solution of Sb^{III} and Sb^{V} ¹⁵ because the thiol groups as “soft acid” has a high affinity
64 for “soft” Sb^{III} ions and a low affinity for “hard” Sb^{V} ions. The objective of this work is to
65 take advantage of mercapto-functionalized silica (MPS) as the DGT binding agents for the
66 selective measurement of Sb^{III} species. MPS has been previously used as a DGT binding
67 agent for As^{III} ,¹⁶ methylmercury¹⁷. However, it has not been investigated for the selective
68 measurement of Sb^{III} by DGT. In this work, the validation of MPS-based DGT device
69 (MPS-DGT) for the measurement of Sb^{III} and the influence of a range of pH (3–8) and
70 electrolyte concentrations (0.0001–0.7 mol L⁻¹ as NaNO_3) on its performance were
71 investigated. Finally, the application for the measurement of Sb^{III} in water was assessed.

72 2. Experimental section

73 2.1 Reagents, materials, and solutions

74 All experimental and reagent solutions were prepared with deionized water. Sb^{III} standard was
75 obtained as potassium antimonyl tartrate (Aldrich, 99.95% purity). The stock solutions of Sb^{III}
76 (1000 mg L⁻¹) and Sb^{V} (1000 mg L⁻¹) were prepared by potassium antimonyl tartrate and
77 potassium hexahydroxyantimonate (Sigma-Aldrich), respectively. The working solutions
78 were prepared by series dilution of the stock solutions immediately prior to their use.
79 Polyethersulfone membrane (PES, pore diameter 0.2 μm , Φ 25 mm, thickness 165 \pm 5 μm) was
80 obtained from Kenker, USA. MPS (200–400 mesh), acrylamide, ammonium peroxydisulfate,
81 bis-acrylamide, tetramethylethylenediamine (TEMED) were purchased from
82 Sigma-Aldrich. The patented agarose-derived cross-linker was purchased from DGT Research
83 Ltd., UK. The other chemicals were obtained from Sinopharm Chemical Reagent Co., Ltd.,
84 Shanghai, China. All chemicals used in this work were of analytical grade and used without

85 further purification. Plastic containers and glassware were cleaned by soaking in diluted
86 HNO₃ (10%) and were rinsed with deionized water prior to use. All the metal stock solutions
87 (1000 mg L⁻¹) were obtained from the National Research Center for Standard Materials
88 (NRCSM, Beijing, China).

89 2.2 Preparation of binding layer

90 MPS binding layer was prepared as described previously.^{16,17a} 1 g of dry mass of MPS was
91 added per 10 mL of pre-gel solution (15% acrylamide and 0.3% DGT cross-linker). 70 μL of
92 10% freshly prepared ammonium persulfate and 25 μL TEMED were added, and the mixture
93 was stirred well before casting. The mixture solution of gel was cast between two glass plates
94 and placed in an oven at 45 °C for 1 h, afterwards the binding gel was peeled off. It required
95 careful handling to avoid breakage. The 2.5 cm diameter disks of binding gel was cut and
96 stored in deionized water. The thickness of hydrated gels was 0.50±0.05 mm.

97 2.3 Uptake and digestion

98 Uptake of disks of MPS binding gel for Sb^{III} was investigated in batch experiments. 10 mL of
99 aqueous solutions containing different initial concentrations of Sb^{III} (0.1, 0.5, and 1 mg L⁻¹)
100 and 0.01 mol L⁻¹ NaNO₃ at pH 5 were equilibrated with individually exposing the discs of
101 binding gel (n=5) for at least 24 h, and then the disks were taken to determine the mass of
102 Sb^{III} remaining in solution. The uptake efficiency of the disks of binding gel for Sb^{III} was
103 calculated as the following equations:

$$104 E_{\text{uptake}} (\%) = 100C_i/C_f \quad (1)$$

105 where E_{uptake} represents the uptake efficiency (%); C_i and C_f are the initial and final
106 concentrations of Sb^{III} (mg L⁻¹) in solution, respectively. The Sb^{III} adsorbed onto the disks of
107 MPS binding gel was carried out in a microwave acid digestion unit (Microwave Digestion
108 System Start D, Milestone, Sorisole, Italy). A disk of MPS binding gel was put into PTFE
109 vessels, and 3 mL of suprapure concentrated HNO₃, 2 mL of suprapure concentrated HCl, and

110 2 mL of HF were added. The digestion was allowed to 1200 W of potency and 140 °C over 30
111 min and then maintained at 140 °C for 45 min. After digestion, the digested solutions were
112 filtered and transferred into a 25 mL volumetric flask, and the volume was completed with a
113 1% solution of HCl (v/v). The digestion efficiency of Sb^{III} from the disks of MPS binding gel
114 was calculated by the following equations:

$$115 \quad E_{\text{digestion}} (\%) = \frac{100C_{\text{digestion}}V_{\text{digested}}}{(C_i - C_f)V_{\text{initial}}} \quad (2)$$

116 where $E_{\text{digestion}}$ represents the digestion efficiency (%); V_{digested} and V_{initial} are the volumes of
117 digested solution of disk and initial solution of Sb^{III}, respectively. A similar procedure was
118 followed for the uptake and digestion efficiencies of Sb^V.

119 **2.4 Assembly of DGT samplers**

120 Pistons and caps were washed in 10% (v/v) HNO₃ and then rinsed nine times with deionized
121 water before use. MPS settled on one side of the gel in the forming process, and this side was
122 placed facing up when assembled in DGT devices. The binding gel was covered by PES
123 membranes. The front cap was pressed tightly. Samplers were sealed in plastic bags and
124 stored at 4 °C.

125 **2.5 Measurement of diffusion coefficients**

126 PES membranes were immersed in 1 mol·L⁻¹ HNO₃ for 24 h before being thoroughly rinsed
127 with deionized water until the pH approached 7, then stored in 0.01 mol·L⁻¹ NaNO₃ until use.
128 By storing PES membranes in NaNO₃ it served to pre-wet the membrane, which aided
129 assembly and facilitated expansion of the membrane.¹⁸ The diffusion coefficients of Sb^{III} ions
130 through the PES membrane in 0.01 mol·L⁻¹ NaNO₃ were determined using a specially
131 designed diffusion cell as described by Zhang et al.¹⁹ The diffusion cell comprised two 150
132 mL of compartments with an interconnecting 20 mm diameter opening. A 25 mm diameter of
133 PES membrane known thickness was placed on the opening, provided the only connection for
134 mass transport between two compartments and allowed the diffusion of Sb^{III} ions from a

135 source solution containing high concentration into a receiving solution which initially
136 contains no Sb^{III} ions. 150 mL of $0.01 \text{ mol L}^{-1} \text{ NaNO}_3$ containing 100.0 mg L^{-1} of Sb^{III} ions
137 with pH at 5 as a source solution was put into compartment A, and 150 mL of 0.01 mol L^{-1}
138 NaNO_3 with the same pH as receiving solution was put into compartment B. The high
139 concentration (100.0 mg L^{-1}) of Sb^{III} ions in compartment A was used to ensure that the
140 concentration depletion of metal ions during diffusion process was negligible. Both
141 compartments were stirred continuously at 300 rpm using an overhead stirrer. Samples were
142 taken from both compartments (50 μL for compartment A and 100 μL for compartment B
143 with the same volume of the corresponding original solution replaced in each compartment) at
144 15 min intervals up to 90 min and measured by AFS. The measurements were repeated for
145 five times. In order to test the influence of a diffusive boundary layer (DBL) on the diffusion
146 coefficients of Sb^{III} through PES membrane, the different stirring rates from 50 to 500 rpm
147 were performed in the source solution. Here, the experimentally determined values of
148 diffusion coefficients, D , were calculated using Eq. (3):

$$149 \quad D = M \cdot \Delta g / A \cdot C \cdot t \quad (3)$$

150 M is the diffusion mass of Sb^{III} ions from a source solution with analyte concentration (C) into
151 receiving solution, after passing through a diffusive layer of area (A) and thickness (Δg) over
152 a deployment time (t). The diffusion coefficient of Sb^{III} ions at different temperatures can be
153 corrected according to Stokes-Einstein equation.²⁰

$$154 \quad \frac{D_1 \eta_1}{T_1} = \frac{D_2 \eta_2}{T_2} \quad (4)$$

155 where D_1 and D_2 are diffusion coefficients at absolute temperature T_1 and T_2 , respectively. η_1
156 and η_2 are viscosities of water at T_1 and T_2 , respectively.

157

158 **2.6 Accumulation over time**

159 To estimate accumulation and measurement of Sb^{III} species over time by MPS–DGT, five sets

160 of triplicate DGT devices were deployed in 40 L of a well-stirred 0.01 mol L⁻¹ of NaNO₃
161 solution spiked with 100 µg L⁻¹ of Sb^{III} at 25 °C. The triplicate probes were removed at 24, 48,
162 72, 96 and 120 h, while grab samples of deployment the solution were taken at each time
163 point and the concentration of Sb^{III} in the solution were measured by AFS as well as for
164 changes in speciation. The MPS–DGT devices are validated by testing the relationship
165 between the mass of analyte accumulated in the binding layer (*M*) and the deployment time (*t*)
166 with a solution of known concentration. *C*_{DGT} is the concentration measured by the DGT
167 technique in solution and can be predicted by the DGT equation:

$$168 \quad M = D \cdot A \cdot C_{\text{DGT}} \cdot t / \Delta g \quad (5)$$

169 where, *A* is diffusive layer of area and Δg is diffusive layer of thickness. The experimental
170 procedures were repeated with Sb^V to confirm that MPS binding agent would not accumulate
171 Sb^V from solution.

172 2.7 Effects of pH, ionic strength and foreign ions

173 To test the effects of solution pH on the performance of MPS–DGT, fifteen replicates of DGT
174 devices were deployed in 30 L of NaNO₃ solutions (0.01 mol L⁻¹) spiked with 100 µg L⁻¹ of
175 Sb^{III} in the pH range 3–8 at 25 °C over periods of time from 24 to 120 h with a 24–hour
176 interval. The pH was adjusted as required using dilute HCl or KOH. The effect of ionic
177 strength of solution on the performance of DGT was investigated by adjusting the ionic
178 strength of a Sb^{III} solution (100 µg L⁻¹) via the addition of NaNO₃. The ionic strengths of the
179 deployment solutions were range from 0.001 to 0.7 mol L⁻¹ (0.001, 0.005, 0.01, 0.05, 0.1, 0.2
180 and 0.7 mol L⁻¹). Most natural waters fall into this range.^{17a} DGT devices were deployed in
181 30 L of continuously stirred Sb^{III} solutions with different concentrations of NaNO₃ at pH 5 for
182 120 h with a 24–hour interval. To investigate the effect of the foreign ions on the uptake of
183 Sb^{III}, MPS–DGT devices were deployed in 40 L of a well-stirred 100 µg L⁻¹ Sb^{III} of solution
184 containing different foreign ions at 25 °C for 120 h with a 24–hour interval. The foreign ions

185 and their concentrations in this study are listed in Table 1. The deployment solution was
186 equilibrated overnight to obtain a stable pH or ionic strength.

187 **2.8 Application to waters in the laboratory**

188 The validation of the MPS–DGT were investigated by deploying DGT devices in 30 L of 0.45
189 μm -filtered natural waters or etching wastewater spiked with $100 \mu\text{g L}^{-1} \text{Sb}^{\text{III}}$ for 24, 48, 72,
190 96 and 120 h. Grab samples of bulk solution were taken at the beginning and in the end of
191 each deployment. The concentrations of Sb^{III} and total Sb were measured. Prior to
192 deployment of DGT devices, the colloidal material which had coagulated during sample
193 storage was removed from solution by filtering. The natural waters and industrial wastewater
194 were immediately pre-filtered under vacuum through qualitative filter papers before filtering
195 through a $0.45 \mu\text{m}$ cellulose nitrate membrane in the laboratory. Major cation concentrations,
196 dissolved organic carbon (DOC) and pH of mine wastewater were also shown in Table 2. The
197 concentrations of DOC were measured using a Dohrmann DC-190 TOC analyzer (USA).

198 **2.9 Detection limit of DGT method**

199 The detection limit of DGT method was determined by calculating 3 times the standard
200 deviation (3σ) of three DGT binding gel blanks and applying Eq. 5 for specific time frames (1
201 day, 3 days, 5 days and 7 days).²¹

202 **2.10 Antimony analysis**

203 A commercial two channel hydride generation nondispersive atomic fluorescence
204 spectrometer (AFS, Model AFS-2202E, Beijing Haiguang Instrument Co., Beijing, China)
205 equipped with a quartz argon–hydrogen flame atomizer, a quartz gas–liquid separator, and
206 coded high intensity hollow cathode lamps of Sb were used for the measurement of Sb^{III} and
207 total Sb concentrations in solution according to the steps described by Deng et al..²² The
208 concentration of Sb^{III} in solution was determined directly by AFS. The total concentration of
209 Sb^{III} and Sb^{V} in solution was measured as follow: In 10 mL aliquot of filtered sample, 2 mL

210 of KI stock solution, 2 mL of 8-hydroxyquinoline stock solutions and 11 mL of HCl (conc.)
211 were added to obtained a 25 mL of final solution.²² This solution was put aside for 20 min at
212 room temperature, and then determined by AFS. The concentration of Sb^V was obtained by
213 subtracting Sb^{III} from the total inorganic Sb of Sb^{III} and Sb^V.

214 3. Results and discussion

215 3.1 Uptake and digestion

216 The uptake efficiencies of MPS binding gel disks for Sb^{III} from 0.1, 0.5, and 1 mg L⁻¹ Sb^{III}
217 solution were >99%, while the uptake efficiencies of Sb^V from 0.1, 0.5, and 1 mg L⁻¹ Sb^V
218 solution were 8.4±4.6, 9.3±3.8 and 10.5±3.2 %. These results indicate that MPS binding gel
219 disks can selectively quantitative accumulate Sb^{III} from aqueous solution. Previous studies
220 have observed the selective adsorption of Sb^{III} by thiol-functionalized sorbents due to the
221 strong interactions of Sb^{III} with the thiolate sulfur.^{14a,23} Accurate calculation of Sb^{III} by
222 MPS–DGT requires the quantitative and reproducible recovery of metal ions captured in MPS
223 binding gels. Concentrated acids digest and destroy the structure of the gels, with complete
224 release of Sb^{III} from the binding gels disks. Prior to analysis of Sb by AFS, parts of the
225 polyacrylamide re-precipitated, making a filtration or centrifugation step necessary.¹³ The
226 high acid matrix does not affect the measurement of AFS for Sb^{III} or Sb^V. The values of
227 $E_{\text{digestion}}$ for Sb^{III} or Sb^V by MPS binding gels disks were 97.7±2.6 and 98.1±3.3 % (mean
228 value ± standard deviation), respectively, which was very close to the digestion efficiency of
229 the precipitated ferrihydrite containing gel described by Luo and co-workers.¹² The low
230 standard deviations indicated that the digestion procedure was reproducible.

231 3.2 Diffusion coefficient in the PES membrane

232 The DGT-labile concentration is accurately determined relying on the use of diffusion
233 coefficient. For Sb^{III}, applying the Stokes–Einstein equation for temperature correction (Eq.
234 4), the diffusion coefficient obtained from Eq 3 in PES membrane was $(3.05±0.09)×10^{-6}$ cm²

235 s^{-1} at pH 5 and temperature 25 °C. There are no published diffusion coefficient data for Sb^{III}
236 measured using a diffusion cell. For Sb^V , the diffusion coefficient measured using a diffusion
237 cell $((1.71 \pm 0.15) \times 10^{-6} \text{ cm}^2 \text{ s}^{-1})$ is $\sim 19\%$ of the diffusion coefficients in water $(9.05 \times 10^{-6}$
238 $\text{ cm}^2 \text{ s}^{-1})$ ²⁴ at 25 °C and lower than the value reported by Panther et al. $(6.04 \pm 0.12) \times 10^{-6} \text{ cm}^2$
239 s^{-1} ¹² and published by Öterlund et al. $(5.55 \pm 0.20) \times 10^{-6} \text{ cm}^2 \text{ s}^{-1}$ ²⁵. The differences might
240 arise from the composition variations of diffusion layers.

241 The diffusion coefficient of Sb^{III} is independent on pH in a 0.01 mol L^{-1} of $NaNO_3$ matrix (as
242 shown in Figure 1a). There are only small discrepancies of diffusion coefficient at the
243 different pH values. For a constant pH 5, the diffusion coefficient of Sb^{III} in PES membrane
244 was independent of ionic strength in the range of 1–200 mmol L^{-1} and decreased at the ionic
245 strength of 700 mmol L^{-1} (as shown in Figure 1b), indicating that the high ionic strengths had
246 effects on the diffusion of Sb^{III} through PES membrane as a result of the change of solution
247 viscosity and/or the competition diffusion between Sb^{III} and nitrate.

248 In poorly moving waters, the DBL thickness becomes significant compared with the diffusive
249 layer thickness. This need arises as a result of the diffusion coefficient of metal ions in bulk
250 solution being similar to the diffusion coefficients in the polyacrylamide gels.⁸ The diffusive
251 gradient within the DBL can also limit the overall mass transport. With the PES membrane
252 diffusive layer described here, changing rates of stirring from 50 to 500 rpm had virtually no
253 influence on the diffusion coefficients of Sb^{III} through PES membrane in the diffusion
254 experiments (Figure 1c). These experimental results indicate that a DBL does not become
255 significant, even in slower moving waters and the transport across the membrane is the
256 rate-limiting step even under the most critical conditions because the diffusion coefficient in
257 the membrane is lower than the diffusion coefficient in the bulk solution. Although the
258 diffusion coefficient of Sb^{III} in aqueous solution has not been reported in the literature,
259 diffusion coefficient of $7.0 \times 10^{-6} \text{ cm}^2 \text{ s}^{-1}$ for Sb^{III} in 1 mol L^{-1} of HNO_3 solution has been

260 previously reported.²⁶ The diffusion coefficients of metals have been significantly affected by
261 ionic strengths of solution and decrease with the increase of ionic strengths.^{8,27} In this work,
262 the same trend has been obtained. We may speculate that the diffusion coefficients of Sb^{III} in
263 natural freshwater may be greater than the diffusion coefficients in 1 mol L^{-1} of HNO_3
264 solution. Diffusion coefficient of Sb^{III} in PES membrane will always be lower than the
265 diffusion coefficient of the metal ions in solution, the formation of a DBL layer at the
266 membrane interface will usually have a very minor contribution to the overall mass transport.
267 This means the thickness of the membrane can be used as Δg in the DGT equation under
268 most deployment conditions without needing to correct for the DBL thickness.

269 **3.3 Accumulation over time**

270 The MPS–DGT was validated by examining the relationship between the mass of Sb^{III}
271 accumulated in MPS and the deployment time with a Sb^{III} or Sb^{V} solution with fixed
272 concentration. The measured mass of Sb^{III} accumulated by MPS–DGT increased linearly with
273 deployment time over 120 h ($R^2=0.9973$) and fitted the theoretical line which calculated from
274 the known solution concentrations (Figure 2). Based on these data, the concentrations of Sb^{III}
275 were calculated using Eq. (5). The fraction of labile Sb^{III} in synthetic solution was $94.5 \pm 3.2\%$
276 of the soluble Sb^{III} concentration, where free species dominated, however, the linear uptake of
277 Sb^{V} with time is not observed by MPS–DGT (Figure 2). This result is consistent with the low
278 uptake efficiency of MPS for Sb^{V} , suggesting that accumulation of Sb^{V} is limited by
279 thermodynamic factors.²⁸ Previous studies have observed the weak coordination interactions
280 of Sb^{V} by thiol groups.²⁹ These results partially confirm that the new MPS–DGT devices
281 meets the assumptions of the DGT equation, ensuring that the concentration of analyte at the
282 interface between the binding gel and diffusive layer was effectively zero. These results
283 confirm that MPS can be used as an appropriate DGT binding agent for the selective
284 accumulation of Sb^{III} .

285 3.4 Effect of pH

286 In order to test the effect of the solution pH on the uptake of Sb^{III} by MPS binding gel,
287 MPS–DGT devices were deployed in synthetic solution at different pH from 3 to 8. Figure 3a
288 shows the ratio of DGT-measured concentrations (C_{DGT}) to the independently measured
289 concentrations of the bulk solutions (C_{SOLN}) over a range of pH values. The results showed
290 that the uptake of Sb^{III} by MPS-DGT devices was satisfactory in pH range of 3–8, indicating
291 that the change of bulk solution pH did not significantly affect the uptake performance of Sb^{III}
292 by MPS-DGT. The pH of natural fresh waters normally falls into this range.

293 3.5 Effect of Ionic Strength

294 To visualize the effect of the ionic strength on uptake of Sb^{III} by MPS–DGT, the ratios of
295 $C_{\text{DGT}}/C_{\text{SOLN}}$ is plotted versus the log value of the ionic strength. At ionic strengths range from
296 0.001 to 0.7 mol L^{-1} , the values of C_{DGT} for Sb^{III} were close to C_{SOLN} (Figure 3b). This
297 suggests that varying the ionic strength of the solution over 3 orders of magnitude did not
298 have a substantial effect on the uptake of Sb^{III} by the MPS–DGT.

299 3.6 Interference Test

300 MPS gel probably also retain other elements besides Sb^{III} in water samples, such as Zn^{II} , Cu^{II} ,
301 Pb^{II} , Cd^{II} and As^{III} .³⁰ The results illustrated in Table 1 show that with one exception, the ratios
302 of $C_{\text{DGT}}/C_{\text{SOLN}}$ were in the range of 0.9–1.1. The presence of Ca^{II} , Mg^{II} , Cd^{II} , Zn^{II} , Pb^{II} , Cu^{II} ,
303 As^{III} and Sb^{V} ions in the sample solution had no obvious influence on the uptake of
304 MPS–DGT for Sb^{III} under the selected conditions due to the thermodynamically strong
305 interactions between Sb^{III} ions and thiol groups.^{14a} Thus, MPS-DGT device clearly offers a
306 high selectivity for Sb^{III} ions.

307 3.7 Detection limit

308 The standard deviation of Sb^{III} blank values for 3 DGT binding gels was 0.05 μg . The
309 detection limit for each DGT mass is, therefore, 0.15 μg ($3 \times 0.05 \mu\text{g}$). Using Eq 5 with a

310 standard DGT configuration (3.14 cm² exposure window area, 110 μm diffusive gel), and
311 assuming a pH of 5 and temperature of 25 °C, the method detection limits (MDL) for DGT
312 over time frames of 1 day, 3 days, 5 days and 7 days are 1.99, 0.664, 0.498, and 0.285 ng L⁻¹,
313 respectively. As the environmental concentration of Sb^{III} is likely to be in the ng/L range, the
314 data show that low ng L⁻¹ detection limits can be achieved for the deployment time at least 3
315 days.

316 **3.8 Performance in spiked waters**

317 To evaluate the performance of the DGT method for the uptake of dissolved inorganic Sb^{III} in
318 waters, DGT devices were deployed in natural freshwater and an etching wastewater spiked
319 with Sb^{III}. No Sb^{III} could be detected in the river water and etching wastewater by direct
320 measurement of AFS, and hence samples were spiked with aliquots of Sb^{III} to give a Sb^{III}
321 concentration of ~100 μg L⁻¹. Reproducibility of MPS–DGT in the spiked waters was very
322 good, with relative standard deviations of less than 6%. For etching wastewater, the value of
323 C_{DGT}/C_{SOLN} (0.95±0.05) between 0.9 and 1.1 is obtained, indicating that the fraction of
324 dissolved inorganic Sb^{III} measured by MPS–DGT is in good agreement with the added Sb^{III}
325 concentration, and MPS–DGT can quantitatively measure the concentration of dissolved
326 inorganic Sb^{III} in etching wastewater over the 5 day deployment. Such good agreement
327 indicates that the coexisting ions in etching wastewater have no influence on the uptake of
328 dissolved inorganic Sb^{III} by MPS–DGT. For natural freshwater, C_{DGT} (58.1±3.4 μg L⁻¹) is
329 significantly lower than C_{SOLN} (90.2±4.2 μg L⁻¹). It is possible that the speciation of added
330 Sb^{III} have be changed by the presence of natural organic matter (such as humic acid) in the
331 natural freshwater, which may be affecting the uptake of MPS–DGT for dissolved inorganic
332 Sb^{III} due to the interactions between Sb^{III} ions and natural organic matter.³¹ Buschmann et al.
333 ³² report that over 30 % of total Sb^{III} may be bound to natural organic matter under
334 environmentally relevant conditions. Tella and Pokrovski found that Sb^{III} can form complexes

335 with the natural organic matter having O- and N-functional groups and 35% of total dissolved
336 Sb^{III} binds to aqueous natural organic matter via carboxylic and hydroxy-carboxylic groups.³³
337 The MPS–DGT estimates are in a good agreement with the literature values. On the other
338 hand, prior to direct AFS measurements, samples were filtered through a 0.22 μm pore-size
339 membrane and acidified. Acidification may release Sb^{III} binding with natural organic matter
340 which remain in the sample, and contributing to the higher value of C_{SOLN} than C_{DGT} . Thus,
341 these results obtained in spiked waters demonstrate the potential and robustness of MPS–DGT
342 to assess Sb^{III} in common water.

343 4. Conclusions

344 In this study, a reliable DGT device with MPS as the binding agents and PES membranes as
345 the diffusion layer was developed for the selective measurement of Sb^{III} in aquatic system.
346 This paper presents the first published measurements of the diffusion coefficient of Sb^{III} in
347 PES membranes. The change in diffusion coefficient at high ionic strength of 0.7 mol L^{-1}
348 NaNO_3 is possibly due to the change of solution viscosity or the competition diffusion. Over
349 the pH range of 3–8 and ionic strengths from 0.001 to 0.7 mol L^{-1} , the mass of Sb^{III}
350 accumulated by MPS–DGT agreed well with the mass of Sb^{III} which predicted from the
351 known solution composition. Furthermore, the presence of cations at concentrations up to 1–3
352 fold higher than those in synthetic solution, has no significant influence on the uptake of Sb^{III}
353 by MPS-DGT. The precision of the results from replicate DGT devices were generally higher
354 than 90%. The competition adsorption between Sb^{III} and Hg^{II} onto MPS affects the
355 accumulation of Sb^{III} by MPS–DGT. When MPS-DGT was applied to spiked etching
356 wastewater in the laboratory, a good agreement was obtained between the C_{DGT} and C_{SOLN} . In
357 spiked natural freshwaters, C_{DGT} is significant lower than C_{SOLN} due to interactions between
358 Sb^{III} ions and natural organic matter. This work has demonstrated that the suitability of
359 MPS–DGT for the measurement of inorganic Sb^{III} species in natural waters is likely to be

360 useful for the assessment of Sb^{III} availability in natural waters. Future research may involve
361 testing the suitability of MPS–DGT to assess Sb^{III} in water under field conditions and
362 determine whether DGT assessment of Sb^{III} matches with availability in waters.

363 Acknowledgements

364 The project was sponsored by the National Natural Science Foundation of China (grant no.
365 21107076 and 21477082), by Liaoning Natural Science Foundation Combined with Open
366 Foundation of Shenyang National Laboratory for Materials Sciences (grant no. 2015021019),
367 and by program for Liaoning Excellent Talents in University of China (grant no.
368 LJQ2015050).

369 References

- 370 1. USEPA, Water Related Fate of the 129 Priority Pollutants, USEPA: Washington, DC, **1979**,
371 Vol. *I*.
- 372 2. Inaba, S.; Takenaka, C. *Environ. Int.* **2005**, *31*, 603–608.
- 373 3. Fan, Z. *Microchim. Acta* **2005**, *152*, 29–33.
- 374 4. (a) Fillela, M.; Belzie, N.; Chen, Y.-W. *Earth-Sci. Rev.* **2002**, *57*, 125–176. (b) He, M.C.;
375 Yang, J.R. *Sci. Total Environ.* **1999**, *243*, 189–196.
- 376 5. Davison, W.; Zhang, H. *Nature* **1994**, *367*, 546–548.
- 377 6. (a) Li, W.; Wang, F.; Zhang, W.; Evans, D. *Anal. Chem.* **2009**, *81*, 5889–5895. (b) Xu, D.;
378 Chen, Y.; Ding, S.; Sun, Q.; Wang, Y.; Zhang, C. *Environ. Sci. Technol.* **2013**, *47*,
379 10477–10484. (c) Tian, Y.; Wang, X.; Luo, J.; Yu, H.; Zhang, H. *Environ. Sci. Technol.* **2008**,
380 *42*, 7649–7654.
- 381 7. Zhang, H.; Davison, W. *Anal. Chem.* **1995**, *67*, 3391–3400.
- 382 8. Li, W.; Teasdale, P.R.; Zhang, S.; John, R.; Zhao, H. *Anal. Chem.* **2003**, *75*, 2578–2583.
- 383 9. Dong, J.; Fan, H.; Sui, D.; Li, L.; Sun, T. *Anal. Chim. Acta* **2014**, *822*, 69–77.
- 384 10. Lerner, B.L.; Seen, A.J. *Anal. Chim. Acta* **2005**, *539*, 349–355.
- 385 11. Garmo, Ø.A.; Røyset, O.; Steinnes, E.; Flaten, T.P. *Anal. Chem.* **2003**, *75*, 3573–3580.
- 386 12. Luo, J.; Zhang, H.; Santner, J.; Davison, W. *Anal. Chem.* **2010**, *82*, 8903–8909.
- 387 13. Panther, J.G.; Stewart, R.R.; Teasdale, P.R.; Bennett, W.W.; Welsh, D.T.; Zhao, H. *Talanta*
388 **2013**, *105*, 80–86.
- 389 14. (a) Sun, H.; Yan, S.C.; Cheng, W.S. *Eur. J. Biochem.* **2000**, *267*, 5450–5457. (b) Ozturk,
390 I.I.; Kourkoumelis, N.; Hadjikakou, S.K.; Manos, M.J.; Tasiopoulos, A.J.; Butler,
391 I.S. Balzarini, J.; Hadjiliadis, N. *J. Coord. Chem.* **2011**, *64*, 3859–3871.
- 392 15. (a) Shakerian, F.; Dadfarnia, S.; Shabani, A.M.H.; Ahmadabadi, M.N. *Food Chem.* **2014**,
393 *145*, 571–577. (b) López-García, I.; Rivas, R.E.; Hernández-Córdoba, M. *Talanta* **2011**, *86*,

- 394 52–57.
- 395 16. Bennett, W.W.; Teasdale, P.R.; Panther, J.G.; Welsh, D.T.; Jolley, D.F. *Anal. Chem.* **2011**,
396 *83*, 8293–8299.
- 397 17. (a) Gao, Y.; Craemer, S.D.; Baeyens, W. *Talanta* **2014**, *120*, 470–474. (b) Liu, J.; Feng, X.;
398 Qiu, G.; Anderson, C.W.N.; Yao, H. *Environ. Sci. Technol.* **2012**, *46*, 11013–11020.
- 399 18. Lerner, B.L.; Seen, A.J. *Anal. Chim. Acta* **2005**, *539*, 349–355.
- 400 19. Scally, S.; Davison, W.; Zhang, H. *Anal. Chim. Acta* **2006**, *558*, 222–229.
- 401 20. Dorsey, N.E. Properties of ordinary water-substance in all its phases: water-vapor/water
402 and all ices; Reinhold Pub. Co.: New York, **1940**.
- 403 21. Lucas, A.; Rate, A.; Zhang, H.; Salmon, S.U.; Radford, N. *Anal. Chem.* **2012**, *84*,
404 6994–7000.
- 405 22. Deng, T.-L.; Chen, Y.-W.; Belzile, N. *Anal. Chim. Acta* **2001**, *432*, 293–302.
- 406 23. (a) Fukuda, H.; Tsunoda, J.; Matsumoto, K.; Terada, K.; Bunseki Kagaku **1987**, *36*,
407 683–687. (b) Yu, M.-Q.; Liu, G.-Q.; Jin, Q.-H. *Talanta* **1983**, *30*, 265–270. (c) Asaoka, S.;
408 Takahashi, Y.; Araki, Y.; Tanimizu, M. *Anal. Sci.* **2011**, *27*, 25–28.
- 409 24. Öterlund, H.; Chlot, S.; Faarinen, M.; Widerlund, A.; Rodushkin, I.; Ingri, J.; Baxter, D.C.
410 *Anal. Chim. Acta* **2010**, *682*, 59–65.
- 411 25. Li, Y.H.; Gregory, S. *Geochim. Cosmochim. Acta* **1974**, *38*, 703–714.
- 412 26. Schoenleber, J.; Stein, N.; Boulanger, C. *J. Electroanal. Chem.* **2014**, *724*, 111–117.
- 413 27. Chen, H.; Sun, T.; Sui, D.; Dong, J. *Anal. Chim. Acta* **2011**, *698*, 27–35.
- 414 28. Jain, V.K.; Bohra, R.; Mehrotra, R.C. Structure and Bonding in Organic Derivatives of
415 Antimony(V), Structure and Bonding 52, Springer-Verlag Berlin Heidelberg, **1982**, 148–196.
- 416 29. Ma, C.; Zhang, Q.; Sun, J.; Zhang, R. *J. Organomet. Chem.* **2006**, *691*, 2567–2574.
- 417 30 (a) Celis, R.; Hermosian, M.C.; Cornejo, J. *Environ. Sci. Technol.* **2000**, *34*, 4593–4599. (b)
418 Jaber, M.; Miché-Brendlé, J.; Michelin, L.; Delmotte, L.; *Chem. Mater.* **2005**, *17*, 5275–5281.

- 419 (c) Spuches, A.M.; Kruszyna, H.G.; Rich, A.M.; Wilcox, D.E. *Inorg. Chem.* **2005**, *44*,
420 2964–2972.
- 421 31. Pilarski, J.; Waller, P.; Pickering, W. *Water, Air, Soil Pollut.* **1995**, *84*, 51–59.
- 422 32. Buschmann, J.; Sigg, L. *Environ. Sci. Technol.* **2004**, *38*, 4535–4541.
- 423 33. Tella, M.; Pokrovski, G.S. *Geochim. Cosmochim. Acta* **2009**, *73*, 268–290.

424 **Figure captions**

425 Figure 1. Diffusion coefficient as a function of pH (a) and ionic strength (b). Data has been
426 adjusted using eq 4 for temperature of 25 °C. Error bars represent the standard deviation of
427 repeated experiments.

428 Figure 2. Dependence of mass of Sb^{III} and Sb^V accumulated by MPS–DGT on deployment
429 time. The dashed line is the theoretical slopes calculated from known concentrations of Sb^{III}
430 in solution.

431 Figure 3. (a) Effect of pH on the performance of MPS–DGT, assessed by the ratio of C_{DGT} to
432 C_{SOLN} , accounting for the change with pH at 25 °C. Ionic strength was kept at 0.01 mol L⁻¹ for
433 all experiments. (b) Effect of ionic strengths on the performance of MPS–DGT at pH 5 at 25
434 °C. Mean values and error bars of triplicate measurements are given. The solid lines indicate
435 $\pm 10\%$ of the C_{DGT}/C_{SOLN} ratio.

436

Table 1 Effects of the foreign ions on the uptake of Sb^{III} by MPS–DGT

Foreign Ions	Concentrations of foreign ions (mg L ⁻¹)	Tolerance ratios (C _{foreign ions} /C _{SbIII})	C _{DGT} (μg L ⁻¹)	C _{SOLN} (μg L ⁻¹)	Ratios of C _{DGT} /C _{SOLN}
Ca ^{II}	100	1000	98.7±2.4	100.8±1.1	0.98±0.03
Mg ^{II}	100	1000	99.8±2.3	100.5±1.2	0.99±0.03
Cd ^{II}	1	10	96.9±2.4	100.1±1.1	0.97±0.03
Zn ^{II}	1	10	96.4±2.0	99.8±0.8	0.97±0.02
Cu ^{II}	1	10	93.5±3.1	100.5±1.0	0.93±0.04
Pb ^{II}	1	10	95.1±2.9	100.8±0.8	0.94±0.03
Ni ^{II}	1	10	99.8±2.5	98.8±0.8	1.01±0.03
As ^{III}	0.1	1	94.7±2.2	99.8±1.8	0.95±0.03
As ^{III}	1	10	92.1±3.2	100.1±1.8	0.92±0.04
Sb ^V	0.1	1	98.2±2.3	103.4±3.1	0.95±0.03
Sb ^V	1	10	96.8±2.8	105.4±3.4	0.92±0.03

437

438

439

Table 2 Major cation concentrations, dissolved organic carbon and pH value of the Hun river water and etching wastewater^a

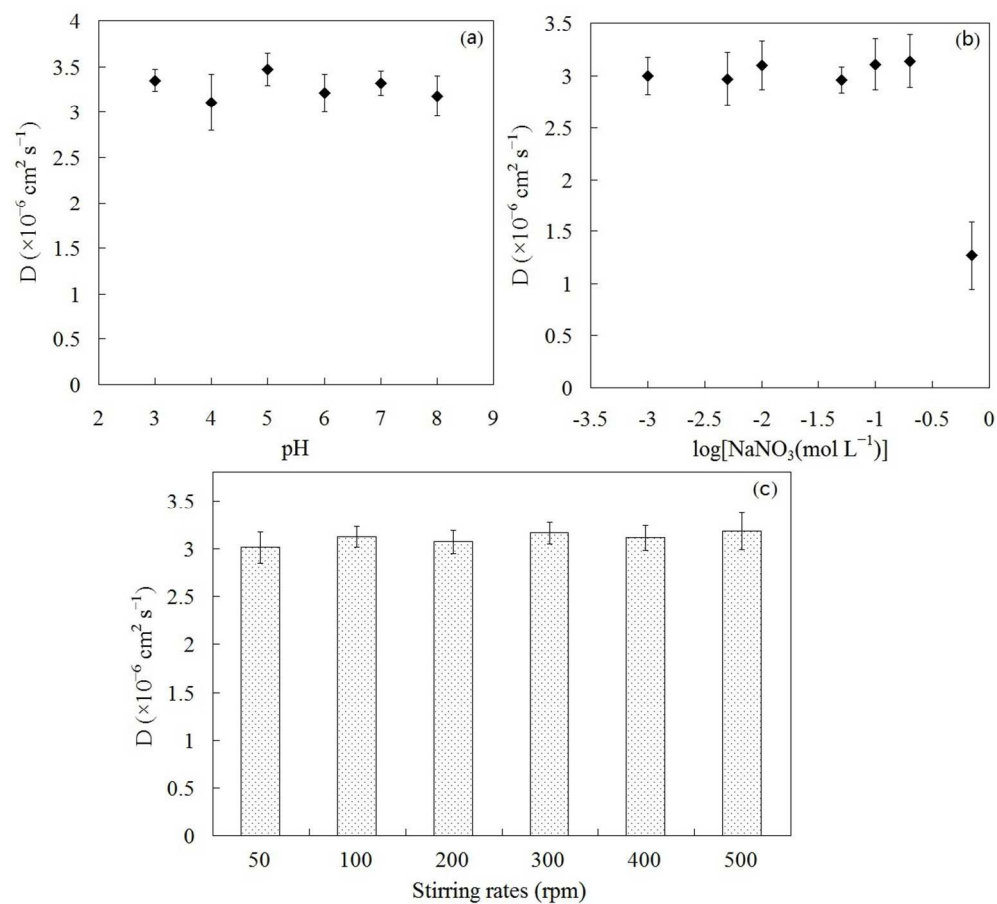
Measured parameters	Water samples	
	Hun river water	Etching wastewater
[K ^I]/mg L ⁻¹	7.8±1.1	2.1±0.6
[Na ^I]/mg L ⁻¹	38.4±8.2	20.9±7.3
[Ca ^{II}]/mg L ⁻¹	62.5±2.5	25.5±2.1
[Mg ^{II}]/mg L ⁻¹	19.7±1.1	8.8±1.0
[Cd ^{II}]/mgL ⁻¹	N.D.	2.1±0.2
[Cu ^{II}]/mgL ⁻¹	N.D.	58.8±0.2
[Pb ^{II}]/mgL ⁻¹	N.D.	32.7±0.3
[Sb ^{III}]/mgL ⁻¹	N.D.	N.D.
[DOC]/ mg C L ⁻¹	8.7±0.8	0.7±0.3
pH	7.3±0.1	4.6±0.1

440

^a Major cation concentrations were measured by FAAS after appropriate dilution except Sb.

441

^b N.D. means not detected.



329x297mm (96 x 96 DPI)

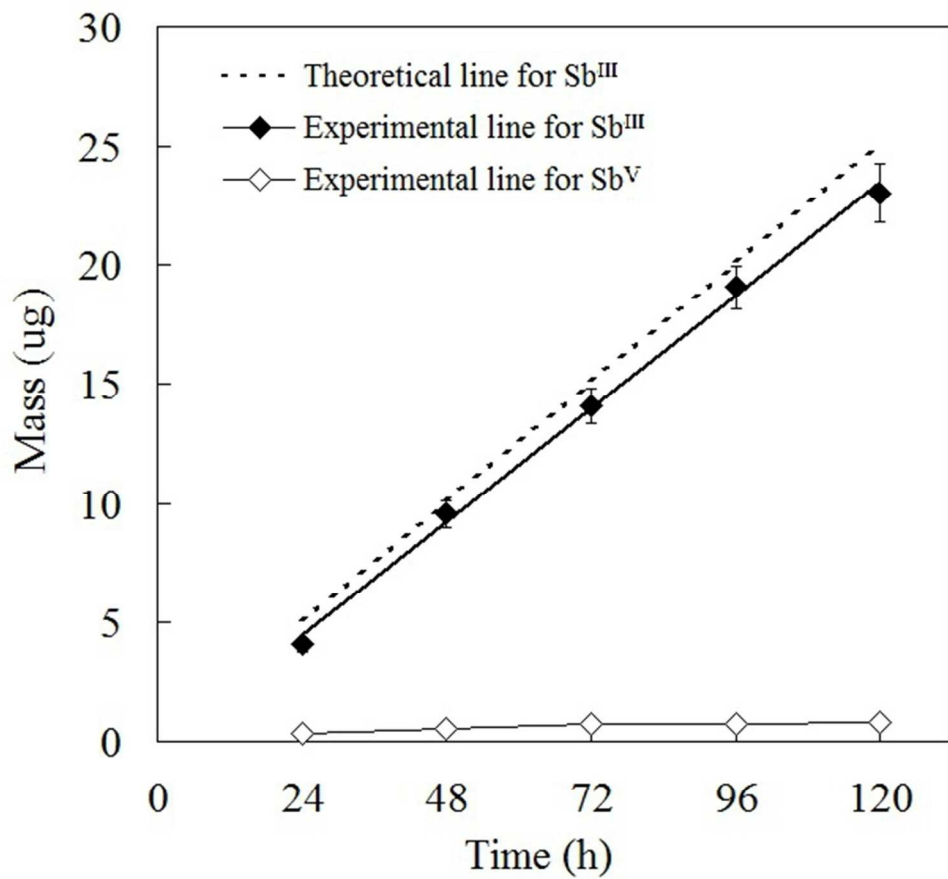


Figure 2. Dependence of mass of Sb^{III} and Sb^V accumulated by MPS-DGT on deployment time. The dashed line is the theoretical slopes calculated from known concentrations of Sb^{III} in solution.
168x148mm (96 x 96 DPI)

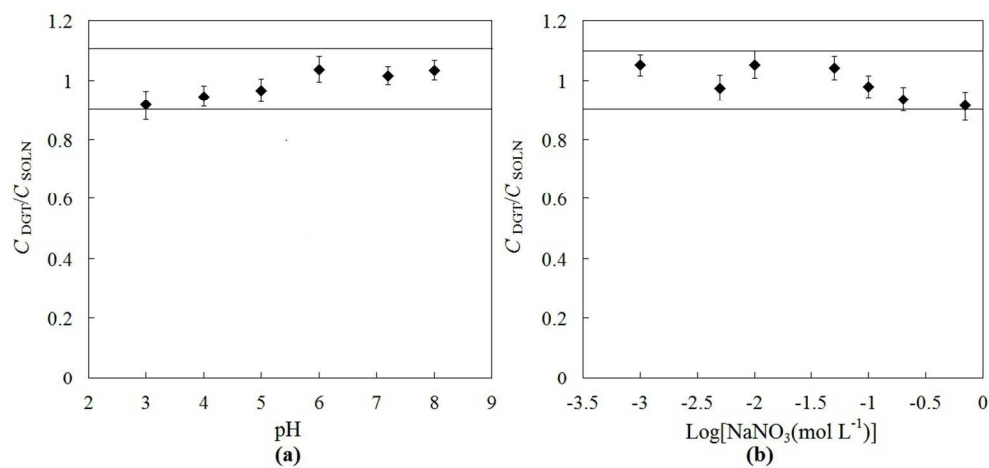
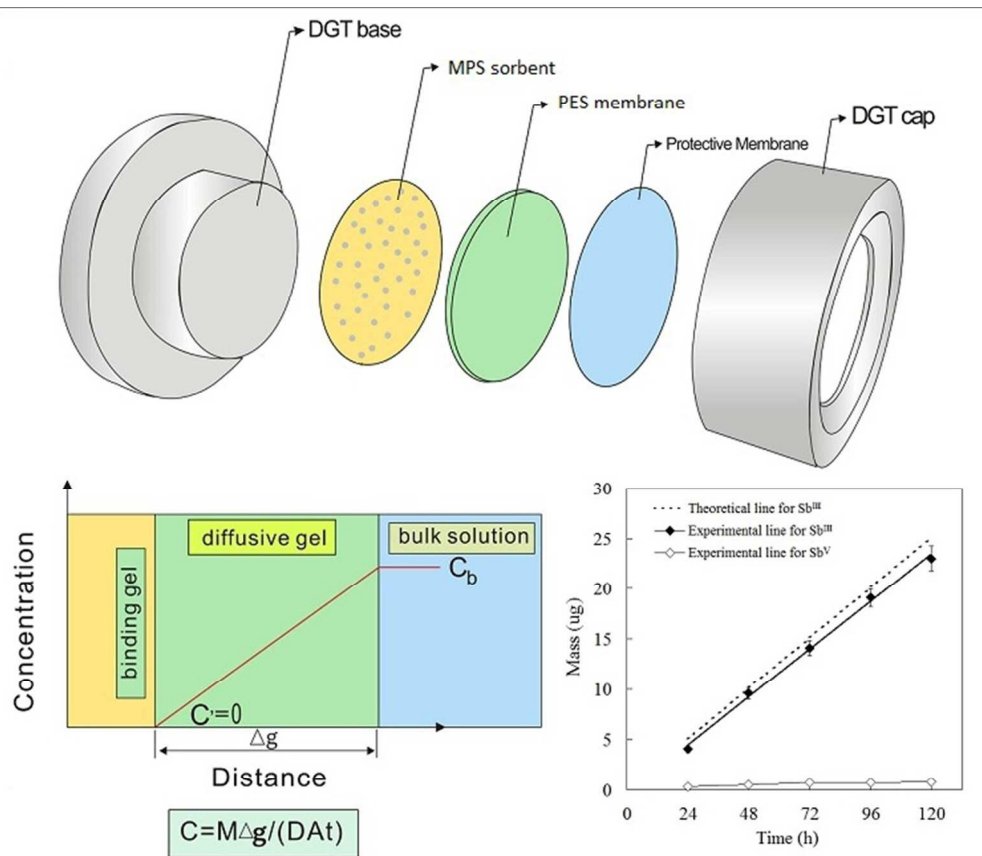


Figure 3. (a) Effect of pH on the performance of MPS-DGT, assessed by the ratio of CDGT to CSOLN, accounting for the change with pH at 25 °C. Ionic strength was kept at 0.01 mol L⁻¹ for all experiments. (b) Effect of ionic strengths on the performance of MPS-DGT at pH 5 at 25 °C. Mean values and error bars of triplicate measurements are given. The solid lines indicate $\pm 10\%$ of the CDGT/CSOLN ratio.
341x159mm (96 x 96 DPI)



Graphical Abstract
67x58mm (285 x 285 DPI)